HHS Public Access

Author manuscript

Nat Immunol. Author manuscript; available in PMC 2012 January 01.

Published in final edited form as:

Nat Immunol. ; 12(7): 647–654. doi:10.1038/ni.2033.

A Cascade of Protein Kinase C Isozymes Promotes Cytoskeletal Polarization in T Cells

Emily J. Quann[1], **Xin Liu**[1], **Grégoire Altan-Bonnet**[2], and **Morgan Huse**[1]

[1] Immunology Program, Memorial Sloan-Kettering Cancer Center, New York, NY 10065

[2] Computational Biology Program, Memorial Sloan-Kettering Cancer Center, New York, NY 10065

Abstract

Polarization of the T cell microtubule-organizing center (MTOC) toward the antigen-presenting cell is driven by the accumulation of diacylglycerol at the immunological synapse (IS). The mechanisms that couple diacylglycerol to the MTOC are not known. Using single-cell photoactivation of the T cell receptor, we demonstrated that three distinct protein kinase C (PKC) isoforms are recruited by diacylglycerol to the IS in two steps. PKC-ε and PKC-η accumulated first in a broad region of membrane, while PKC-θ arrived later in a smaller zone. Functional experiments indicated that PKC-θ was required for MTOC reorientation, and that PKC-ε and PKC-η operated redundantly to promote PKC-θ recruitment and subsequent polarization responses. These results establish a previously uncharacterized role for PKCs in T cell polarity.

The formation of an immunological synapse (IS) between a lymphocyte and a target cell is coupled to the polarization of the lymphocyte's microtubule-organizing center (MTOC) to a position adjacent to the IS[1, 2]. MTOC reorientation establishes an axis of polarity that enables T cells and natural killer cells to secrete cytokines and cytolytic factors in a directional manner toward the target cell, and thereby maintain the specificity of their effector responses. Alignment of the microtubule cytoskeleton with the IS may also promote asymmetric cell division, which is thought to be important for the acquisition of T cell memory[3].

MTOC polarization is driven by the coupling of activated cell surface receptors to cytosolic regulators of the cytoskeleton. In T cells, recognition by the T cell receptor (TCR) of major histocompatibility complex (MHC) molecules bearing cognate peptide induces the recruitment of the microtubule motor protein dynein[4-6]. Microtubules extend outward from the MTOC, and it is thought that synaptically anchored dynein mediates polarization by pulling on these microtubules to reel the MTOC toward the IS. A number of TCR-proximal tyrosine kinases and scaffolding proteins have been implicated in MTOC reorientation[6-9].

Correspondence should be addressed to M.H. (husem@mskcc.org).

Contributions

E. J. Q. and M. H. designed the experiments. E. J. Q. collected and analyzed the data. X. L. performed the Marcksl1 experiments. G. A.-B. assisted with Matlab programming and data analysis. M. H. wrote the manuscript with help from E. J. Q. and G. A.-B.

Precisely how early signals from these proteins are linked to dynein recruitment, however, remains largely unknown. Using a high-resolution photoactivation and imaging approach, we showed recently that the synaptic accumulation of diacylglycerol (DAG), a lipid second messenger produced by phospholipase C-γ (PLC-γ), is necessary for both dynein recruitment and MTOC reorientation downstream of the TCR[6]. We also demonstrated that intracellular calcium (Ca^{2+}), another second messenger generated by PLC-γ, is not required for the polarization response.

DAG plays a central role in a number of signaling pathways, most often by recruiting molecules that contain DAG-binding C1 domains. Conspicuous among these are members of the protein kinase C (PKC) family of serine-threonine kinases, which participate in a variety of important signaling pathways in multiple cell types[10]. PKCs are classified into one of three subfamilies: conventional PKC (cPKC) isoforms (PKC-α, -β, and -γ) require both Ca^{2+} and DAG for activation, novel PKC (nPKC) isoforms (PKC-δ, -ε, -η, and -θ) require DAG but not Ca^{2+}, and atypical PKC (aPKC) isoforms (PKC-λ/τ and -ζ) require neither DAG nor Ca^{2+}, and are instead regulated by protein-protein interactions.

Multiple PKC isozymes, including members of all three subfamilies, have been implicated in various aspects of cell polarity and directional migration in many cell types[11-15]. It remains largely unclear, however, whether and how PKCs contribute to MTOC polarization in T cells. That the T cell response requires DAG, but not Ca^{2+}, indicates that nPKCs, rather than cPKCs or aPKCs, are more likely to be involved. Of these, PKC-δ was recently shown to be dispensable for MTOC polarization, although it is required for the secretion of cytolytic granules in $CD8^+$ T cells[16, 17]. By far the best-studied nPKC isoform in T cells is PKC-θ, which is necessary for TCR-induced activation of several key transcription factors[18, 19], and has also been implicated in the upregulation of integrin-dependent adhesion[20]. Although there is no direct evidence that PKC-θ is involved in MTOC reorientation, it is recruited to the center of the IS before the arrival of the MTOC[21]. PKC-θ is also required for T cells to “break symmetry” when plated on stimulatory bilayers[22], indicating that it may play a role in the establishment of cell polarity in certain contexts. Far less is known about PKC-ε and PKC-η. PKC-ε-deficient mice display no obvious defect in T cell activation[23], suggesting that the protein is either unimportant or that it is functionally redundant with another nPKC. Within the nPKC subfamily, PKC-ε is most closely related to PKC-η (60% identity for PKC-ε vs. PKC-η, ~40% for PKC-ε vs. PKC-δ or PKC-θ), while PKC-θ is most closely related to PKC-δ (60% identity for PKC-θ vs. PKC-δ, 40-45% for PKC-θ vs. PKC-ε or PKC-η). It is therefore not unreasonable to expect some redundancy between PKC-ε and PKC-η, although this possibility has not been explored.

By combining TCR photoactivation and single cell imaging with targeted loss-of-function, we analyzed all four nPKC proteins in the context of T cell MTOC polarization. We found that PKC-θ, PKC-ε, and PKC-η were all recruited to the IS prior to reorientation of the MTOC. PKC-ε and PKC-η arrived first and accumulated in a broad region of the plasma membrane, while PKC-θ arrived later and adopted a more localized pattern. Consistent with the notion that PKC-ε and PKC-η function redundantly with each other but nonredundantly with PKC-θ, siRNA-mediated suppression of PKC-ε and PKC-η together was required to inhibit MTOC polarization, while suppression of PKC-θ alone was sufficient to impair the

response. We also demonstrated that PKC-ε and PKC-η are required for accumulation of PKC-θ, suggesting that they prime the IS for PKC-θ recruitment. Taken together, these results indicate that an ordered cascade of nPKCs functions downstream of DAG to promote MTOC reorientation in T cells.

Results

nPKCs accumulate in the region of TCR activation

To analyze the molecular mechanisms of MTOC reorientation, we use a live imaging approach in which polarization responses are triggered in individual T cells using a localized pulse of ultraviolet (UV) light[24]. Primary $CD4^+$ T cell blasts expressing the 5C.C7 TCR, which is specific for a moth cytochrome c (MCC) peptide presented by the MHC protein $I\text{-}E^K$, are attached to coverslips coated with a photoactivatable version of the peptide-MHC (pMHC). Focused UV light is then used to create a micron-sized region of active pMHC beneath an individual T cell, followed by the imaging of intracellular signaling and cytoskeletal responses using various fluorescent probes. This approach enables us to control the stimulation of MTOC reorientation both spatially and temporally, and to monitor responses in the plasma membrane at high resolution using total internal reflection fluorescence (TIRF) microscopy.

Given the importance of synaptically localized DAG for MTOC reorientation, we hypothesized that nPKCs, which contain high affinity C1 domains, would be recruited to the IS and play a role in the polarization response. Using RT-PCR, we demonstrated that all PKC family members, with the exception of PKC-γ, are expressed in murine $CD4^+$ T cells (**Supplementary Fig. 1**). To investigate whether TCR signaling induces the recruitment of any of these proteins to the region of receptor stimulation, we performed photoactivation experiments using T cells expressing red fluorescent protein (TagRFP-T)-labeled tubulin together with various full-length PKC isoforms fused to green fluorescent protein (GFP). TagRFP-T was used as the red fluorophore in all of our double labeling experiments, and it will be called simply RFP hereafter. Of the four nPKC proteins we examined, PKC-θ, PKC-ε and PKC-η were observed by TIRF microscopy to accumulate in the UV irradiated region, and in all three cases this accumulation preceded reorientation of the MTOC (**Fig. 1a-c** and **Supplementary Movies 1-3**). In contrast, PKC-δ did not accumulate in response to TCR photoactivation, despite the fact that MTOC reorientation to the irradiated region did occur (**Fig. 1d**). Recruitment of PKC-θ, PKC-ε and PKC-η was blocked by the PLC-γ inhibitor U73122, indicating that DAG production was required for these responses (**Supplementary Fig. 2**). TCR photoactivation did not induce the localized enrichment of either PKC-α (a cPKC) or PKC-ζ (an aPKC) (**Supplementary Fig. 3a,b**). While we did observe pulsatile recruitment of PKC-β (a cPKC) to the region of TCR stimulation, this recruitment required Ca^{2+} (**Supplementary Fig. 3c**), which we have demonstrated is not necessary for MTOC polarization[6]. By contrast, the accumulation of PKC-θ, PKC-ε and PKC-η was Ca^{2+} independent (data not shown).

TCR-induced recruitment of PKC-ε and PKC-η had not been reported previously and was somewhat surprising. Hence, to confirm these results we imaged T cells expressing fluorescently labeled nPKC isoforms as they formed conjugates with APCs. We observed

robust accumulation of PKC-θ, PKC-ε and PKC-η at the IS, but little to no recruitment of PKC-δ (**Supplementary Fig. 4**), consistent with the results of the photoactivation experiments. We conclude that TCR stimulation triggers the synaptic accumulation of PKC-θ, PKC-ε and PKC-η.

Different nPKCs adopt distinct accumulation patterns

We next compared the spatial and temporal properties of PKC-θ, PKC-ε and PKC-η recruitment by analyzing cells that expressed all possible pairwise combinations of the three kinases. Cursory examination of the photoactivation experiments suggested that PKC-θ accumulation was more tightly localized to the irradiated zone than either PKC-ε or PKC-η (**Fig. 2a** and **Supplementary Movies 4, 5**). To quantify these apparent differences in localization, we calculated the two-dimensional autocorrelation function for each image, and derived a width parameter for this function after Gaussian fitting[25]. We then determined the ratio of width parameters (width ratio) for each pair of nPKCs for every image. The ratios relating PKC-ε to PKC-η clustered closely around 1, indicating that the two kinases displayed similarly sized accumulation patterns (**Fig. 2b**). In contrast, the ratios relating either PKC-ε or PKC-η with PKC-θ tended to be larger than 1 (by an average of 20-25%) (**Fig. 2b**). These results confirmed that PKC-ε and PKC-η were indeed recruited to broader plasma membrane domains than PKC-θ in response to TCR photoactivation.

We also examined the localization of PKC-θ, PKC-ε and PKC-η during IS formation on supported lipid bilayers. T cells expressing Lifeact–RFP, a probe for filamentous actin[26], together with GFP-labeled PKC-θ, PKC-ε, or PKC-η were imaged by TIRF microscopy on bilayers containing agonist pMHC and the adhesion molecule ICAM. Consistent with previous studies[22, 27], we observed actin enrichment in a ring at the periphery of the IS. PKC-θ accumulation was fully contained within this actin ring (**Supplementary Fig. 5a**). Quantification confirmed that the region of PKC-θ accumulation was consistently smaller than the area delimited by actin (**Supplementary Fig. 5b**). In contrast, PKC-ε and PKC-η were recruited evenly over the entire synaptic membrane, and their accumulations were roughly equivalent in size with the actin ring (**Supplementary Fig. 5b-d**). Hence, PKC-ε and PKC-η also occupy broader membrane domains than PKC-θ in the context of the IS.

To quantify and compare the kinetics of PKC-θ, PKC-ε and PKC-η accumulation, we calculated the crosscorrelation functions[6] relating the recruitment of each protein with either the recruitment of the other nPKCs or the reorientation of the MTOC during photoactivation experiments. This analysis confirmed that each of the three nPKCs accumulated at the irradiated region prior to MTOC reorientation (**Fig. 2c**). Consistently, PKC-ε and PKC-η recruitment was observed to precede PKC-θ recruitment by 5-10 seconds (**Fig. 2c, d**). In contrast, pairwise comparison of PKC-ε and PKC-η accumulation revealed little to no difference in kinetics (**Fig. 2e**). Hence, PKC-ε and PKC-η are recruited simultaneously, and their recruitment precedes PKC-θ.

DAG binding by nPKCs is mediated by the tandem C1 domains located N-terminal to the kinase domain[10]. To determine the extent to which the scope and kinetics of nPKC recruitment depended solely on the C1 region, we imaged T cells expressing fluorescently labeled tandem C1 domains from PKC-ε or PKC-η together with their full-length nPKC

counterparts. Crosscorrelation and autocorrelation analyses indicated that the C1 domain constructs largely recapitulated the recruitment behavior of their respective full-length proteins (**Supplementary Fig. 6**). In the case of PKC-θ, we observed a small but reproducible difference in both the scope and kinetics of accumulation, suggesting that determinants outside of the tandem C1 region had some effect on the recruitment behavior of full-length PKC-θ. Nevertheless, these deviations were small relative to the differences we observed between full-length PKC-θ and the other full-length nPKCs (**Fig. 2**). Hence, we conclude that nPKC recruitment behavior at the synapse is, for the most part, dictated by the tandem C1 domain region of each protein.

TCR signaling induces localized PKC activity

To determine whether the recruitment of PKC-θ, PKC-ε and PKC-η is associated with enhanced PKC enzymatic activity in the region of TCR stimulation, we employed a fluorescently labeled reporter construct containing Marcksl1, a well-characterized PKC substrate. Unphosphorylated Marcksl1 binds to the plasma membrane, but it is released into the cytosol by PKC-mediated phosphorylation[28]. Hence, the depletion of Marcksl1 from the membrane can be used to assess localized PKC activity.

When expressed in T cells, GFP- or RFP-labeled Marcksl1 accumulated in the plasma membrane, where it could be visualized by TIRF microscopy. Photoactivation of the TCR induced the depletion of Marcksl1 from the irradiated zone prior to MTOC reorientation (**Fig. 3a, b** and **Supplementary Movie 6**). This depletion response was impaired by U73122, a PLC-γ inhibitor, and by Gö6983, a broad-specificity PKC inhibitor, indicating that DAG production and PKC activity, respectively, are both required (**Supplementary Fig. 7a**). Furthermore, a Marcksl1 mutant bearing Ser to Ala mutations at the consensus PKC phosphorylation sites (Marcksl1-mut) remained membrane-associated under these conditions (**Supplementary Fig. 7b**), consistent with the idea that PKC activity drives Marcksl1 depletion. Like nPKC recruitment, release of Marcksl1 from the membrane appeared to predict the location of MTOC polarization (**Fig. 3a,b**), implying a close relationship between PKC activity and the MTOC.

To establish the kinetics of Marcksl1 depletion relative to nPKC recruitment, we imaged Marcksl1–RFP together with PKC-η–GFP or PKC-θ–GFP. Crosscorrelation analyses revealed Marcksl1 depletion to be closely associated with the recruitment of both kinases. Consistently, however, PKC-η was observed to arrive concurrently with or to slightly precede Marcksl1 depletion, with PKC-θ recruitment occurring shortly after (**Fig. 3c**). These results suggest that PKC-η and PKC-ε mediate the early depletion of Marcksl1, and further support the notion that PKC-θ is recruited to the region of TCR stimulation at a later time.

PKC activity is required for MTOC polarization

The observed recruitment of nPKCs to the region of TCR stimulation suggested that PKC activity might be important for MTOC reorientation. To test this hypothesis, we analyzed polarization responses in the presence of Gö6983. In TCR photoactivation experiments, Gö6983 inhibited MTOC reorientation at relatively low concentrations (500 nM) (**Fig. 4a**). Quantification of the data revealed that the average root mean square distance between the

MTOC and the irradiated region was substantially larger in Gö6983-treated cells, indicative of a polarization defect. Gö6983 also inhibited MTOC reorientation to the IS in T cell–APC conjugates (**Fig. 4b,c**). Importantly, we observed robust antigen-dependent Ca^{2+} flux in conjugate experiments, implying that early TCR signaling was unaffected by Gö6983.

If PKC phosphorylation is required for MTOC polarization, one might expect that excess amounts of an off-pathway PKC substrate would hamper the response by diverting enzymatic activity from the appropriate targets. Consistent with this notion, we found that overexpression of Marcksl1 tended to delay MTOC reorientation (**Supplementary Fig. 8**). This effect was not observed in cells expressing Marcksl1-mut, demonstrating that the potential of Marcksl1 to retard polarization correlated with its ability to absorb PKC activity. Taken together, these data indicate that PKC activity is required for MTOC reorientation.

nPKCs are necessary for MTOC polarization

Given that PKC-θ, PKC-ε and PKC-η arrive at the IS prior to the MTOC, they seemed the most likely PKC isoforms to be involved in the polarization response. To assess the importance of each protein, we introduced by nucleotransfection siRNA duplexes specific for each isoform and sometimes two nPKC isoforms into T cells from mice carrying transgenes for both GFP-Centrin-2 (ref. 29) and the 5C.C7 TCR. The MTOC is easily detectable in all T cells derived from these mice, which facilitates data collection considerably.

Knockdown of PKC-θ resulted in an MTOC reorientation defect that could be observed clearly in TCR photoactivation experiments (**Fig. 5a,b**). Conversely, suppression of either PKC-ε or PKC-η in isolation had little to no effect on MTOC reorientation (**Fig. 5a,c**). However, knockdown of both PKC-ε and PKC-η in combination did inhibit the polarization response, suggesting that the two proteins play redundant roles in the pathway (**Fig. 5a,c**). Functional redundancy between PKC-ε and PKC-η, but not between either protein and PKC-θ, is consistent with our observations that the spatiotemporal patterns of PKC-ε and PKC-η accumulation are similar to each other but distinct from that of PKC-θ.

We also examined MTOC reorientation in T cells from PKC-θ knockout[30], 5C.C7 transgenic mice. PKC-θ-deficient T cells polarized poorly in response to photoactivation when compared to wild-type and heterozygous controls, especially in experiments where cells were stimulated with lower intensity UV light (**Fig. 6a**). However, these defects were consistently less substantial than those observed in siRNA knockdown studies, suggesting that compensatory mechanisms exist to counteract the effects of PKC-θ deficiency during T cell development *in vivo*. To confirm that this subtle polarization phenotype was due specifically to loss of PKC-θ, we used retroviral transduction to restore PKC-θ expression in PKC-θ-deficient T cells before subjecting them to TCR photoactivation. Expression of PKC-θ–RFP significantly improved both the speed and fidelity of MTOC reorientation in PKC-θ-deficient T cells (**Fig. 6b**). Importantly, the same construct had little to no effect on polarization responses in wild-type and heterozygous controls, indicating that the defect observed in the mutant cells resulted directly from PKC-θ deficiency. In addition, expression of a catalytically inactive PKC-θ mutant failed to enhance polarization responses in PKC-θ-deficient cells (**Supplementary Fig. 9**), demonstrating that functional PKC-θ was required

for this rescue effect. These experiments, combined with the siRNA knockdown studies described above, demonstrate that PKC-θ, PKC-ε and PKC-η play functionally important roles in MTOC polarization.

PKC-ε and PKC-η promote PKC-θ recruitment

The observation that PKC-ε and PKC-η preceded PKC-θ to the region of TCR stimulation suggested that PKC-ε and PKC-η might play a role in the driving the accumulation of PKC-θ. To test this hypothesis, we analyzed the recruitment of PKC-θ–GFP in T cells treated with siRNA against PKC-ε together with PKC-η. We also performed reciprocal photoactivation experiments in which PKC-η–GFP dynamics were monitored in PKC-θ-suppressed cells. Knockdown of PKC-ε and PKC-η clearly inhibited PKC-θ accumulation relative to non-targeting controls (**Fig. 7a**), indicating that PKC-ε and PKC-η are necessary for optimal PKC-θ recruitment. Interestingly, knockdown of PKC-θ had no effect on the accumulation of PKC-η (**Fig. 7b**), consistent with the notion that PKC-θ functions downstream of PKC-ε and PKC-η in this pathway.

Given that PKC-θ recruitment during MTOC polarization is largely controlled by the tandem C1 region of the protein (**Supplementary Fig. 6**), we examined whether siRNA knockdown of PKC-ε and PKC-η also affected the recruitment of the PKC-θ C1 domains. For these experiments, we used T cells derived from mice expressing a transgene encoding the C1 domains of PKC-θ fused to GFP, together with a transgene for the 5C.C7 TCR. Suppression of PKC-ε together with PKC-η inhibited recruitment of the PKC-θ C1 region to a similar extent as we had observed for the full-length protein (**Fig. 7c**). Accumulation of the tandem C1 probe was also inhibited by Gö6983 (**Supplementary Fig. 10**). Taken together, our results indicate that PKC-ε and PKC-η prime the IS for the recruitment of PKC-θ.

nPKCs are required for T cell effector function

The observation that PKC-ε and PKC-η operate redundantly to promote MTOC polarization suggested that these proteins might also play redundant roles in downstream effector responses. To test this hypothesis, we evaluated cytokine production in T cells transfected with siRNAs against either PKC-θ alone or PKC-ε and PKC-η in combination. PKC-θ is required for T cell interleukin 2 (IL-2) responses[30], and its suppression served as a positive control in these experiments. T cells were stimulated with plate-bound pMHC together with the costimulatory molecule CD80, and the production of IL-2 and interferon-γ (IFN-γ) was quantified by intracellular cytokine staining. Knockdown of PKC-ε together with PKC-η inhibited both IL-2 and IFN-γ responses relative to control cells treated with non-targeting siRNA (**Fig. 8**). In PKC-θ-suppressed cells, we also observed defects in both IL-2 and IFN-γ production, which was somewhat surprising given previous reports indicating that IFN-γ responses are normal in PKC-θ-deficient T cells[31]. This discrepancy probably reflects that fact that we used T_H0 blasts differentiated *in vitro* for our studies rather than effector cells isolated after infection or immunization *in vivo*. Knockdown of PKC-θ alone or PKC-ε together with PKC-η also inhibited cytokine production in response to APCs (data not shown). We conclude that PKC-θ, PKC-ε, and PKC-η all play important roles in the induction of T cell effector responses.

Discussion

In this study, we demonstrated that three nPKC isoforms, PKC-ε, PKC-η, and PKC-θ, function in an ordered cascade to prime the IS for MTOC reorientation. These results establish a previously unappreciated role for nPKCs during IS formation, and provide insight into the dynamic regulation of cell polarity in lymphocytes.

The synaptic localization of PKC-θ and its crucial role in T cell development and signaling have been well established[18, 19, 21]. Hence, it was not particularly surprising for us to find that PKC-θ was recruited to the plasma membrane downstream of TCR stimulation and that it was required for MTOC polarization. However, given previous work indicating that PKC-η is not recruited to the IS[21] and that T cell activation is unaffected in $PKC-\tilde{\varepsilon}\text{deficient}$ mice[23], it was surprising to find that both proteins did indeed accumulate synaptically, and that they were important for MTOC reorientation and downstream effector responses. Previous analyses of PKC-η recruitment were based largely on immunocytochemistry, and it is possible that the antibody used against PKC-η in these experiments was not effective for intracellular staining. Furthermore, the absence of a phenotype in PKC-ε-deficient T cells could simply reflect the redundancy between PKC-ε and PKC-η that we have documented in this study. In that regard, mice lacking both PKC-ε and PKC-η will be useful tools in future studies aimed at assessing the extent to which each protein can compensate for the other in various aspects of T cell function.

Using two-color TIRF imaging, we showed that PKC-ε and PKC-η are recruited to the region of TCR stimulation ~15 seconds before MTOC reorientation and 5-10 seconds before PKC-θ. We also found that PKC-ε and PKC-η accumulate in a broader plasma membrane zone than PKC-θ. This distinction was observed both on glass surfaces containing immobilized photoactivatable pMHC and on supported lipid bilayers containing mobile agonist pMHC and ICAM. Classical studies have divided the mature IS into three distinct supramolecular activation clusters (SMACs), a central SMAC (cSMAC) containing the TCR, a peripheral SMAC (pSMAC) enriched in integrins, and a distal SMAC (dSMAC) defined by the actin ring[32]. Although there is some controversy over whether PKC-θ localizes to the cSMAC or the pSMAC[22, 33], it is generally accepted that its accumulation falls within the dSMAC. This hypothesis is consistent with our bilayer experiments, which showed that PKC-θ was contained by the actin ring at all timepoints. In contrast, PKC-ε and PKC-η were recruited evenly over the entire IS, overlapping extensively with the dSMAC as well as the more central synaptic domains. Taken together, our data indicate that PKC-ε and PKC-η are not constrained with PKC-θ to the center of the IS, and suggest that the determinants that guide their localization are at least partially distinct. It has been reported that signaling from the costimulatory receptor CD28 induces the formation of PKC-θ clusters in a ring around the cSMAC[34]. Interestingly, although we did observe annular PKC-θ clustering in membranes containing pMHC, ICAM and the CD28 ligand CD80, PKC-ε and PKC-η did not form CD28-induced clusters of this kind (E. J. Q. and M. H., unpublished observations).

The spatiotemporal features of PKC-η and PKC-θ accumulation were largely recapitulated by constructs containing the respective tandem C1 domains of each protein, suggesting that

the C1 region is primarily responsible for the observed differences in PKC-θ recruitment relative to PKC-ε and PKC-η. That PKC-ε and PKC-η accumulated faster and in a broader domain than PKC-θ suggests that they may have a higher affinity for DAG. However, it is also possible that PKC-ε and PKC-η, upon arrival at the IS, induce the production of an additional, non-DAG determinant that primes the IS for binding of the PKC-θ C1 region. This determinant could presumably even be non-lipid in nature, given that C1 domains from several PKC isoforms are known to engage in protein-protein interactions in the appropriate environments[35]. In that regard, it is notable that we did not observe recruitment of PKC-δ to the plasma membrane in response to TCR stimulation, despite the fact that PKC-δ binds DAG in other contexts[36]. Indeed, it is likely that DAG binding is only one of a number of features controlling C1 region-dependent nPKC localization in T cells.

The precise mechanisms by which PKC-θ, PKC-ε, and PKC-η promote MTOC reorientation remain to be determined. It is formally possible that PKC-θ alone couples plasma membrane signals to downstream cytoskeletal machinery, and that PKC-ε and PKC-η serve merely to recruit PKC-θ to the IS. We consider this model unlikely, however, in part because the subtle polarization phenotype of PKC-θ-deficient T cells indicates that other pathways can, in the right setting, partially compensate for PKC-θ deficiency. We favor an alternative model in which PKC-ε and PKC-η are coupled to the MTOC in a PKC-θ-independent manner for at least a portion of the response. Given the observed differences in recruitment behavior between PKC-θ, PKC-ε and PKC-η, it is tempting to speculate that PKC-ε and PKC-η are crucial for the initiation of polarization, while PKC-θ contributes during subsequent phases, possibly by refining the positioning of the MTOC at the IS. The identification of nPKC substrates and other associated proteins that function in this context will no doubt shed light on the precise roles played by each nPKC isoform. In that regard, it is intriguing to note that both PKC-ε and PKC-η associate with the formin mDia[37], which has been implicated in MTOC reorientation in T cells[38]. It will be interesting to explore the possibility that mDia acts in concert with the nPKCs to modulate T cell polarity.

Using Marcksl1 as a probe of PKC function, we documented a rise in PKC activity at the IS that was coincident with the recruitment of PKC-ε and PKC-η. Marcksl1 overexpression also imposed a substantial delay in MTOC reorientation, consistent with the idea that PKC activity plays a central role in the process. This delay was quite intriguing to us because Marcksl1 has been shown to associate with dynein through the regulatory dynactin complex[39, 40], and therefore could conceivably play a role in dynein regulation during the polarization response. However, siRNA-mediated suppression of Marcksl1 had no effect on MTOC reorientation (data not shown), indicating Marcksl1 is probably not involved in this process at physiological concentrations.

PKCs are crucial for polarity induction in multiple cell types. However, in adherent cells such as fibroblasts and astrocytes, it is the aPKCs, rather than the nPKCs, that appear to play a central role[11, 15]. aPKCs act together with components of the PAR (partitioning-defective) complex to establish polarity over a period of hours, which is substantially longer than the minutes required for MTOC reorientation in lymphocytes. Interestingly, aPKCs and PAR proteins have been observed to localize asymmetrically in T cell–APC conjugates[3, 41, 42], but only well after MTOC polarization to the IS has occurred. In addition, a recent report

indicated that aPKC activity is required for sustained MTOC polarization (after 30 min) and the delivery of cytokines to the IS[43]. These results, when taken together with our data, suggest that polarity establishment at the IS proceeds in two stages: a rapid, direction sensing phase mediated by lipid second messengers and nPKCs, followed by a consolidation phase that requires aPKCs and PAR proteins. One might imagine that the first stage would be crucial for fast events like cytotoxic killing, while the second stage would be necessary for facilitating slower processes, such as asymmetric cell division. Further identification and characterization of molecules required for the induction and/or the maintenance of lymphocyte polarity should enable us to assess more effectively the contribution of cell polarity to complex immune function.

Supplementary Material

Refer to Web version on PubMed Central for supplementary material.

Acknowledgments

We thank D. Littman (New York University) for PKC-θ-deficient mice; W. Marks and the MSKCC Mouse Genetics Core Facility for assistance with generating the C1–GFP mice; R. Wedlich-Soldner (International Max Planck Research School) for Lifeact-RFP; A. Hall (MSKCC), S. Rotenberg (Queens College), and M. O. Li (MSKCC) for reagents and advice; E. Alonzo (MSKCC) for assistance with functional studies; N. Bantilan (MSKCC) for technical support; S. S. Yi and the MSKCC Microchemistry Core Facility for peptide synthesis; A. Hall for critical reading of the manuscript; and members of the Huse and Li labs for helpful comments. E. J. Q. is supported by a Ruth L. Kirschstein National Research Service Award. Additional support was provided to M. H. by the National Institutes of Health (R01-AI087644), the Searle Scholars program, and the Cancer Research Institute. G.A-B was supported by a grant from the National Institutes of Allergy and Infectious Diseases (R01-AI083408).

Methods

Mice

The animal protocols used for this study were approved by the Institutional Animal Care and Use Committee, Memorial Sloan-Kettering Cancer Center, New York, NY. GFP–Centrin-2 5C.C7 TCR transgenic mice were generated by crossing 5C.C7 αβTCR transgenic *Rag2*$^{-/-}$ mice (Taconic) to GFP–Centrin-2 transgenics (Jackson Labs). Transgenic mice expressing the tandem C1 domains of PKCθ linked to GFP (C1–GFP) were generated by subcloning DNA encoding PKC-θ amino acids 160-281 fused to GFP into pCAGGS/ES downstream of a chicken β-actin promoter. The linearized vector was injected into fertilized eggs (C57BL/6JxCBA/J), and the eggs transferred to pseudopregnant recipients. Mice positive for the transgene were crossed to B10A and then to 5C.C7 αβTCR transgenic mice to generate mice positive for both transgenes. 5C.C7 GFP–Centrin-2 and 5C.C7 C1–GFP mice were genotyped by flow cytometric analysis of GFP, CD4 and CD8 in peripheral blood. *Prkcq*$^{-/-}$ 5C.C7 TCR transgenic mice were generated by breeding *Prkcq*$^{-/-}$ mice with 5C.C7 αβTCR transgenics, and then crossing the heterozygous progeny. PKC-θ deficiency was monitored by PCR using the following oligonucleotides: 5'-TAAGAGTAATCTTCCAGAGC-3' (sense) and 5'-TTGGTTCTCTTGAACTCTGC-3' (antisense) to detect the wild-type locus, and sense and 5'-ACTGCATCTGCGTGTTCGAA-3' for the mutant locus.

Cells

5C.C7 T cell blasts were prepared by mixing lymphocytes from 5C.C7 TCR transgenic mice displaying the appropriate PKC-θ genotype with irradiated splenocytes from B10A mice in a 1:5 ratio with 5 μM MCC peptide. In experiments comparing wild-type, *Prkcq*$^{+/-}$, and *Prkcq*$^{-/-}$ T cells, lymphocytes were derived from littermates. Cells were cultured in RPMI containing 10% FCS. 30 IU/ml IL-2 was added 16 h after lymphocyte isolation and cells were split as needed in RPMI containing 30 IU/ml IL-2. 5C.C7 GFP–Centrin-2 and 5C.C7 C1–GFP T cell blasts were prepared similarly, but both lymphocytes and splenocytes were isolated from the same mice. CH12 cells, which were used as APCs in **Supplementary Fig. 4** and **Fig. 4b-c**, were maintained in RPMI plus 10% FCS.

Signaling probes

The full-length coding sequences of PKC-α, PKC-β, PKC-δ, PKC-η, PKC-θ, PKC-ζ, and Marcksl1 were amplified from 5C.C7 T cell RNA by RT-PCR and ligated into the MSCV retroviral expression vector upstream and in-frame of either GFP or RFP. Full-length mouse PKC-ε was amplified from pUC19 PKC-ε and ligated into MSCV as described above. The tandem C1 domains of PKC-η (amino acids 172-295) were amplified from full-length PKC-η–GFP–MSCV and ligated into the MSCV vector as described above. Lifeact–RFP was subcloned as a single fragment into MSCV. The PKC-θ K409R mutation and the phosphorylation site mutations (S93A and S104A) in Marcksl1 were generated by site directed mutagenesis using the Stratagene protocol. Constructs for RFP–tubulin and the tandem C1 domains of PKC-θ linked to GFP have been described[6]. Constructs were retrovirally transduced into T cells as described[6].

RT-PCR

RNA was isolated from 5C.C7 T cells 7 or 8 d after primary peptide stimulation using TRIZOL (Invitrogen) according to the manufacturer's protocol. The SuperScript One-Step kit (Invitrogen) was used for RT-PCR.

siRNA Nucleofection

2×10^6 5C.C7 primary T cell blasts were nucleofected 5 or 6 d after primary peptide stimulation with 600 pmol siRNA against PKC-θ, PKC-ε, PKC-η, PKC-ε plus PKC-η, or with Non-Targeting (NT) siRNA (Thermo Scientific Dharmacon) using the Amaxa mouse T Cell Nucleofector Kit (Lonza). 3 μg of pmaxFP-Red-C or pmax-GFP reporter plasmid (Lonza) was added to each reaction to identify nucleofected cells. After nucleofection, cells were transferred to RPMI containing 30 IU/ml IL-2 and 1 nM IL-7 and incubated 48 h prior to analysis.

Immunoblotting

Immunoblots were prepared using lysates from equal numbers of nucleofected cells. After blotting, nitrocellulose membranes were blocked in TBS plus 0.1% Tween (TBST) with 5% milk, and probed overnight at 4°C with antibodies for PKC-θ (1:500, Santa Cruz

Biotechnology), PKC-ε (1:1000, BD Transduction Laboratory), or PKC-η (1:400, Santa Cruz Biotechnology). Following incubation in the primary antibody, membranes were washed in TBST, incubated in the appropriate horseradish peroxidase conjugated secondary antibody (1:3000, Cell Signaling), and washed again with TBST. SuperSignal West Pico Chemiluminescent Substrate (Thermo Scientific) was used to detect immunoreactivity. Membranes were re-probed with anti-β-Actin (1:10000, Sigma) as a loading control.

Live Imaging

Live cell imaging was performed on an inverted fluorescence video microscope (Olympus), using Slidebook software for image acquisition. Photoactivation experiments were carried out in minimal imaging medium (MIM, colorless RPMI with 5% FCS) on glass surfaces prepared as previously described[6] using 8-well chamber slides (Nunc) and 0.5 μg/ml NPE-MCC–I-E^k (photoactivatable), 3 μg/ml Hb–I-E^k (nonstimulatory), and 0.5 μg/ml antibody to H-$2K^k$ (BD Biosciences). A Mosaic digital diaphragm (Photonic Instruments) attached to a Mercury HBO lamp (Olympus) was used for photoactivation. TIRF or epifluorescence images were captured every 3 or 5 s over an 8 min period using a 150X, 1.45 NA objective lens (Olympus) together with illumination from 488 nm and 561 nm lasers (Melles Griot) for imaging of GFP and RFP, respectively. Cells were photoactivated for 500 or 1000 ms during the tenth timepoint of the capture series. The MTOC was imaged using epifluorescence illumination and all other probes were imaged in TIRF. Gö6983 (Calbiochem) and U73122 (EMD) were added directly to cells, after the collection of control data, as 2X stocks in MIM to a final concentration of 0.5 μM and 0.6 μM, respectively. For live imaging of T cell–APC conjugates, 5C.C7 GFP–Centrin-2 T cells were loaded with Fura-2 AM, washed with MIM, and incubated in 16-well chamber slides with 0.1% DMSO or 0.5 μM Go6983 for 10 min before the addition of CH12 cells previously pulsed with 1 μM MCC. Fura-2 AM images, differential interference contrast images, and a 20 μm *z*-stack of GFP images were collected every 30 s for 30 min using a 40X objective lens (Olympus). For live imaging of synapse formation, 0.5 μg/ml biotinylated MCC–I-E^k and 1 μg/ml biotinylated ICAM were used to coat streptavidin containing supported lipid bilayers as described[44]. TIRF images of fluorescently labeled T cells in contact with these bilayers were collected every 30 s for 30 min using a 60X, 1.45NA objective lens (Olympus).

Image and Statistical Analysis

Image analysis was performed using Slidebook and Matlab, and results were visualized in Excel and Prism. Polarization of the MTOC during photoactivation experiments was analyzed by calculating the root mean square distance (r.m.s.d.) of the MTOC from the center of the photoactivated region at each timepoint. This data was represented for an entire data set as the average path of the MTOC versus time and also as a polarization histogram. Average paths were determined by calculating the mean r.m.s.d. at corresponding timepoints for an entire collection of cells. Polarization histograms were generated by sorting all of the r.m.s.d. from each cell in the data set for all timepoints during the second half of the time-lapse into 0.2 μm bins. Recruitment or depletion of signaling probes in response to TCR stimulation was analyzed by plotting mean fluorescence intensity at the photoactivated

region versus time after background correction and normalization to the ten timepoints before UV irradiation. Cross-correlation analysis was applied as described[6] using normalized fluorescence intensity curves from paired GFP and RFP channels. Crosscorrelation analysis determines the time delay between a set of paired responses by calculating the overlap between the two responses as one of them is mathematically shifted in time with respect to the other. Two dimensional image autocorrelation analysis, which measures the characteristic scale of dominant features within an image in a manner that is independent of the precise geometry of those features, was implemented in Matlab and combined with Gaussian fitting to determine the characteristic width of a given fluorescent signal. This analysis was applied to background corrected images obtained from cells expressing both GFP and RFP labeled proteins. The distributions of GFP and RFP for each cell were directly compared by calculating the ratio of the distribution widths for the two probes at each timepoint (width ratio). For certain analyses, the mean width ratio for each cell was calculated by averaging the ratios at each timepoint. MTOC polarization in T cell–APC conjugates was quantified by positional assignment of the MTOC into one of four equally spaced bins starting from the IS and moving backward, as described[6]. Analysis of T cell–APC conjugates was blinded. Areas occupied by Lifeact–RFP and GFP-labeled PKC in bilayer experiments were quantified in Slidebook after intensity thresholding. The values from corresponding timepoints were then averaged over all cells in the data set. For each cell, time 0 was set to the first image showing cell spreading.

Cytokine production assays

Stimulatory surfaces were prepared by coating 96-well Immuno plates (Nunc) with 10 μg/ml streptavidin in 0.1 M $NaHCO_3$ for 4 h at 25°C, followed by blocking with 2% BSA in HBS (20 mM HEPES pH 7.5, 150 mM NaCl) for 2 h at 25°C. After washing with HBS, surfaces were left overnight at 4°C in HBS with 2% BSA containing 1 μg/ml CD80, 1 μg/ml Hb–I-E^k, and either 10 ng/ml, 1 ng/ml, 0.1 ng/ml or 0 ng/ml MCC–I-E^k, and then washed again with HBS. 5×10^4 5C.C7 T cells were activated with either these stimulatory surfaces or with 5×10^4 CH12 cells pulsed with 500 nM, 50 nM, 5 nM, or 0 nM MCC. GolgiPlug (BD Biosciences) was added after 1 h to accumulate cytokine intracellularly. After 3.5 h, EDTA was added to a final concentration of 2.5 mM to break up conjugates between T cells and CH12 cells. After an additional 30 min, cells were blocked with 2.4G2 antibody specific for FcγII/III, stained with anti-mouse CD4 APC-eFluor 780 (RM4-5, eBioscience), fixed and permeablized with BD Cytofix/Cytoperm (BD Biosciences), and finally stained with APC Rat Anti-Mouse IL-2 (JES6-5H4, BD Pharmingen) and PE Rat Anti-Mouse IFN-γ (XMG1.2, BD Pharmingen). Flow cytometry was performed using an LSRII analyzer (BD). Only cells expressing GFP (from the pmax-GFP nucleofection marker) were used for analysis.

References

1. Huse M, Quann EJ, Davis MM. Shouts, whispers, and the kiss of death: directional secretion in T cells. Nat Immunol. 2008; 9:1105–1111. [PubMed: 18800163]
2. Stinchcombe JC, Griffiths GM. Secretory mechanisms in cell-mediated cytotoxicity. Annual review of cell and developmental biology. 2007; 23:495–517.

3. Chang JT, et al. Asymmetric T lymphocyte division in the initiation of adaptive immune responses. Science. 2007; 315:1687–1691. [PubMed: 17332376]
4. Combs J, et al. Recruitment of dynein to the Jurkat immunological synapse. Proc Natl Acad Sci U S A. 2006; 103:14883–14888. [PubMed: 16990435]
5. Martin-Cofreces NB, et al. MTOC translocation modulates IS formation and controls sustained T cell signaling. J Cell Biol. 2008; 182:951–962. [PubMed: 18779373]
6. Quann EJ, Merino E, Furuta T, Huse M. Localized diacylglycerol drives the polarization of the microtubule-organizing center in T cells. Nat Immunol. 2009; 10:627–635. [PubMed: 19430478]
7. Kuhne MR, et al. Linker for activation of T cells, zeta-associated protein-70, and Src homology 2 domain-containing leukocyte protein-76 are required for TCR-induced microtubule-organizing center polarization. J Immunol. 2003; 171:860–866. [PubMed: 12847255]
8. Lowin-Kropf B, Shapiro VS, Weiss A. Cytoskeletal polarization of T cells is regulated by an immunoreceptor tyrosine-based activation motif-dependent mechanism. J Cell Biol. 1998; 140:861–871. [PubMed: 9472038]
9. Martin-Cofreces NB, et al. Role of Fyn in the rearrangement of tubulin cytoskeleton induced through TCR. J Immunol. 2006; 176:4201–4207. [PubMed: 16547257]
10. Newton AC. Protein kinase C: poised to signal. Am J Physiol Endocrinol Metab. 2010; 298:E395–402. [PubMed: 19934406]
11. Etienne-Manneville S, Hall A. Cell polarity: Par6, aPKC and cytoskeletal crosstalk. Curr Opin Cell Biol. 2003; 15:67–72. [PubMed: 12517706]
12. Fan J, et al. PKCdelta clustering at the leading edge and mediating growth factor-enhanced, but not ecm-initiated, dermal fibroblast migration. J Invest Dermatol. 2006; 126:1233–1243. [PubMed: 16543902]
13. Rosenberg M, Ravid S. Protein kinase Cgamma regulates myosin IIB phosphorylation, cellular localization, and filament assembly. Mol Biol Cell. 2006; 17:1364–1374. [PubMed: 16394101]
14. Volkov Y, Long A, McGrath S, Ni Eidhin D, Kelleher D. Crucial importance of PKC-beta(I) in LFA-1-mediated locomotion of activated T cells. Nat Immunol. 2001; 2:508–514. [PubMed: 11376337]
15. Suzuki A, Ohno S. The PAR-aPKC system: lessons in polarity. J Cell Sci. 2006; 119:979–987. [PubMed: 16525119]
16. Ma JS, Haydar TF, Radoja S. Protein kinase C delta localizes to secretory lysosomes in CD8+ CTL and directly mediates TCR signals leading to granule exocytosis-mediated cytotoxicity. J Immunol. 2008; 181:4716–4722. [PubMed: 18802074]
17. Ma JS, et al. Protein kinase Cdelta regulates antigen receptor-induced lytic granule polarization in mouse CD8+ CTL. J Immunol. 2007; 178:7814–7821. [PubMed: 17548619]
18. Altman A, Villalba M. Protein kinase C-theta (PKCtheta): it's all about location, location, location. Immunol Rev. 2003; 192:53–63. [PubMed: 12670395]
19. Manicassamy S, Gupta S, Sun Z. Selective function of PKC-theta in T cells. Cellular & molecular immunology. 2006; 3:263–270. [PubMed: 16978534]
20. Letschka T, et al. PKC-theta selectively controls the adhesion-stimulating molecule Rap1. Blood. 2008; 112:4617–4627. [PubMed: 18796635]
21. Monks CR, Kupfer H, Tamir I, Barlow A, Kupfer A. Selective modulation of protein kinase C-theta during T-cell activation. Nature. 1997; 385:83–86. [PubMed: 8985252]
22. Sims TN, et al. Opposing effects of PKCtheta and WASp on symmetry breaking and relocation of the immunological synapse. Cell. 2007; 129:773–785. [PubMed: 17512410]
23. Gruber T, Thuille N, Hermann-Kleiter N, Leitges M, Baier G. Protein kinase Cepsilon is dispensable for TCR/CD3-signaling. Mol Immunol. 2005; 42:305–310. [PubMed: 15589318]
24. Huse M, et al. Spatial and temporal dynamics of T cell receptor signaling with a photoactivatable agonist. Immunity. 2007; 27:76–88. [PubMed: 17629516]
25. Petersen NO, Hoddelius PL, Wiseman PW, Seger O, Magnusson KE. Quantitation of membrane receptor distributions by image correlation spectroscopy: concept and application. Biophysical journal. 1993; 65:1135–1146. [PubMed: 8241393]

26. Riedl J, et al. Lifeact: a versatile marker to visualize F-actin. Nature methods. 2008; 5:605–607. [PubMed: 18536722]
27. Bunnell SC, Kapoor V, Trible RP, Zhang W, Samelson LE. Dynamic actin polymerization drives T cell receptor-induced spreading: a role for the signal transduction adaptor LAT. Immunity. 2001; 14:315–329. [PubMed: 11290340]
28. Arbuzova A, Schmitz AA, Vergeres G. Cross-talk unfolded: MARCKS proteins. The Biochemical journal. 2002; 362:1–12. [PubMed: 11829734]
29. Higginbotham H, Bielas S, Tanaka T, Gleeson JG. Transgenic mouse line with green-fluorescent protein-labeled Centrin 2 allows visualization of the centrosome in living cells. Transgenic research. 2004; 13:155–164. [PubMed: 15198203]
30. Sun Z, et al. PKC-theta is required for TCR-induced NF-kappaB activation in mature but not immature T lymphocytes. Nature. 2000; 404:402–407. [PubMed: 10746729]
31. Marsland BJ, Soos TJ, Spath G, Littman DR, Kopf M. Protein kinase C theta is critical for the development of in vivo T helper (Th)2 cell but not Th1 cell responses. J Exp Med. 2004; 200:181–189. [PubMed: 15263025]
32. Dustin ML. Hunter to gatherer and back: immunological synapses and kinapses as variations on the theme of amoeboid locomotion. Annual review of cell and developmental biology. 2008; 24:577–596.
33. Monks CR, Freiberg BA, Kupfer H, Sciaky N, Kupfer A. Three-dimensional segregation of supramolecular activation clusters in T cells. Nature. 1998; 395:82–86. [PubMed: 9738502]
34. Yokosuka T, et al. Spatiotemporal regulation of T cell costimulation by TCR-CD28 microclusters and protein kinase C theta translocation. Immunity. 2008; 29:589–601. [PubMed: 18848472]
35. Colon-Gonzalez F, Kazanietz MG. C1 domains exposed: from diacylglycerol binding to protein-protein interactions. Biochimica et biophysica acta. 2006; 1761:827–837. [PubMed: 16861033]
36. Stahelin RV, et al. Mechanism of diacylglycerol-induced membrane targeting and activation of protein kinase Cdelta. J Biol Chem. 2004; 279:29501–29512. [PubMed: 15105418]
37. Eng CH, Huckaba TM, Gundersen GG. The formin mDia regulates GSK3beta through novel PKCs to promote microtubule stabilization but not MTOC reorientation in migrating fibroblasts. Mol Biol Cell. 2006; 17:5004–5016. [PubMed: 16987962]
38. Gomez TS, et al. Formins regulate the actin-related protein 2/3 complex-independent polarization of the centrosome to the immunological synapse. Immunity. 2007; 26:177–190. [PubMed: 17306570]
39. Jin T, Yue L, Li J. In vivo interaction between dynamitin and MacMARCKS detected by the fluorescent resonance energy transfer method. J Biol Chem. 2001; 276:12879–12884. [PubMed: 11278693]
40. Yue L, Lu S, Garces J, Jin T, Li J. Protein kinase C-regulated dynamitin-macrophage-enriched myristoylated alanine-rich C kinase substrate interaction is involved in macrophage cell spreading. J Biol Chem. 2000; 275:23948–23956. [PubMed: 10827182]
41. Ludford-Menting MJ, et al. A network of PDZ-containing proteins regulates T cell polarity and morphology during migration and immunological synapse formation. Immunity. 2005; 22:737–748. [PubMed: 15963788]
42. Oliaro J, et al. Asymmetric cell division of T cells upon antigen presentation uses multiple conserved mechanisms. J Immunol. 2010; 185:367–375. [PubMed: 20530266]
43. Bertrand F, et al. Activation of the ancestral polarity regulator protein kinase C zeta at the immunological synapse drives polarization of Th cell secretory machinery toward APCs. J Immunol. 2010; 185:2887–2894. [PubMed: 20679531]
44. Abeyweera TP, Merino E, Huse M. Inhibitory signaling blocks activating receptor clustering and induces cytoskeletal retraction in natural killer cells. J Cell Biol. 2011; 192:675–690. [PubMed: 21339333]

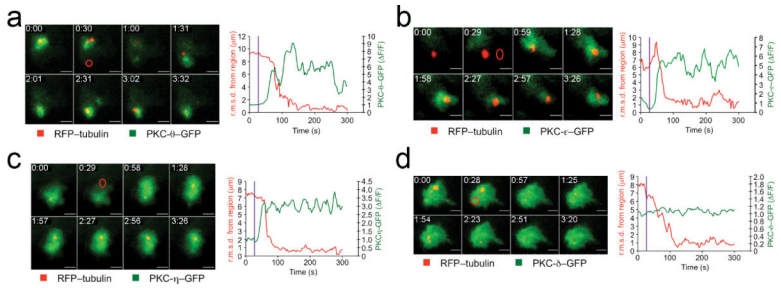

Figure 1.

PKC-θ, PKC-ε, and PKC-η, but not PKC-δ, accumulate at the region of TCR activation prior to MTOC reorientation. 5C.C7 T cells expressing RFP–tubulin together with GFP-labeled PKC-θ (**a**), PKC-ε (**b**), PKC-η (**c**) or PKC-δ (**d**) were imaged on coverslips coated with photoactivatable pMHC and stimulated in defined regions with a pulse of UV light. Throughout the paper, fusion protein names indicate the position of the fluorescent label relative to the protein of interest (e.g. RFP–tubulin = RFP N-terminal to tubulin). In each panel, a representative timelapse montage (~30 s intervals) is shown to the left with the time and position of UV irradiation indicated by a red oval. Corresponding quantification is shown to the right with PKC accumulation expressed as normalized mean fluorescence intensity (ΔF/F) within the irradiated region and MTOC reorientation expressed as root mean square distance (r.m.s.d.) between the MTOC and the irradiated region. UV irradiation is indicated in graphs by a purple line. Throughout the figure, scale bars = 5 μm. All data are representative of at least two independent experiments, with n ≥ 6 cells per experiment.

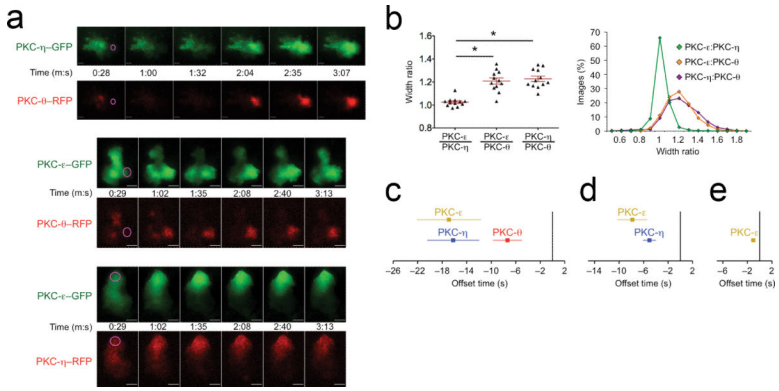

Figure 2.

nPKCs display distinct accumulation patterns and kinetics. TCR photoactivation was performed using 5C.C7 T cells expressing all three pairwise combinations of PKC-θ, PKC-ε, and PKC-η. Each pair of proteins was imaged using TIRF microscopy in two fluorescent configurations (e.g. PKC-θ–GFP with PKC-η–RFP, and PKC-η–GFP with PKC-θ–RFP). (**a**) Timelapse montages (~30 s intervals) showing representative accumulation behavior, with the time and position of UV irradiation events indicated by magenta ovals. Scale bars = 5 μm. (**b**) Left, mean width ratios for each pairwise combination of nPKCs determined after autocorrelation analysis (see **Methods**). Data points represent the average ratio over an entire timelapse (160 timepoints) for one cell. Each data set comprises 12 cells. Asterisks indicate P-values < 0.0001 (Student's T-test). Right, histogram computed using all width ratios from the entire data set. (**c**) Average “offset” times separating the recruitment of PKC-θ, PKC-ε, and PKC-η from MTOC reorientation, determined from cells expressing GFP-labeled PKCs with RFP–tubulin. (**d**) Offset times separating PKC-ε and PKC-η recruitment from PKC-θ recruitment, determined from cells expressing either labeled PKC-ε or PKC-η together with labeled PKC-θ. (**e**) Offset time separating PKC-ε recruitment from PKC-η recruitment, determined from cells expressing labeled PKC-ε with labeled PKC-η. Offset times were calculated using crosscorrelation curves from at least 15 paired responses (see **Methods**). Throughout the figure, error bars = standard error of the mean (s.e.m.). All data are representative of at least two independent experiments.

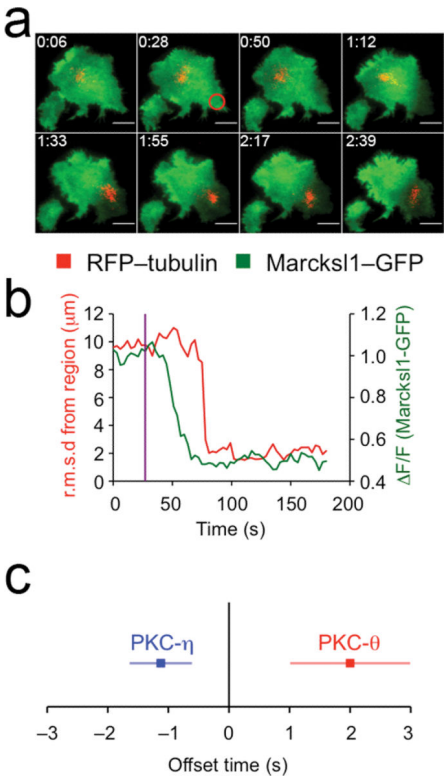

Figure 3.

nPKC recruitment correlates with increased PKC activity. (**a,b**) TCR photoactivation experiments were performed using 5C.C7 T cells expressing Marcksl1–GFP and RFP–tubulin. (**a**) Representative timelapse montage (~20 s intervals), with the time and position of UV irradiation indicated by a red oval. Scale bars = 5 μm. (**b**) Quantification of the response in (**a**), showing Marcksl1–GFP depletion together with MTOC reorientation, presented as described in **Fig. 1**. (**c**) Average offset times separating PKC-η–GFP and PKC-θ–GFP recruitment from Marcksl1–RFP depletion (time 0). Offsets were determined by crosscorrelation analysis of at least 12 paired responses. Error bars = s.e.m. All data are representative of at least two independent experiments, with n ≥ 6 cells per experiment.

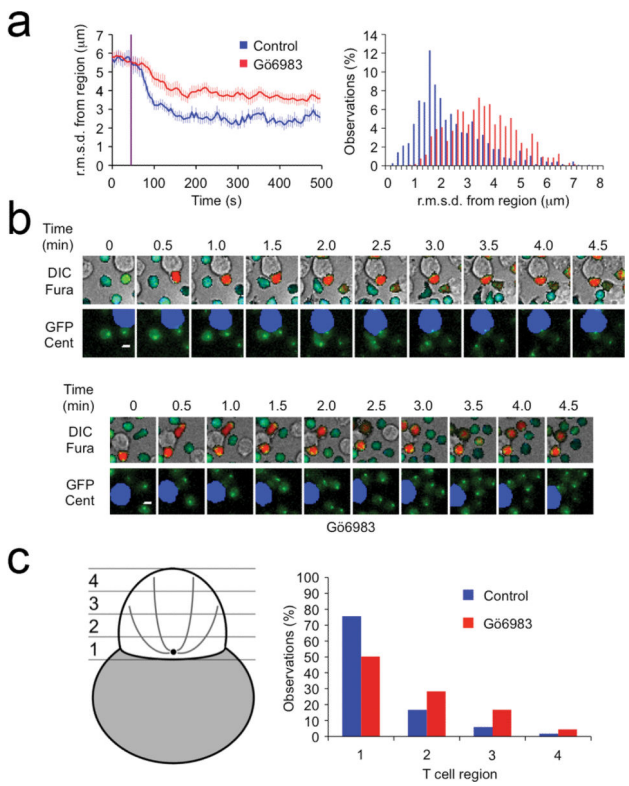

Figure 4.

PKC activity is required for MTOC polarization. (**a**) 5C.C7 T cells expressing GFP–tubulin were photoactivated in the presence or absence of 500 nM Gö6983. Left, average r.m.s.d. between the MTOC and the irradiated region (called the average path) as a function of time. UV irradiation, which occurred after 50 s, is denoted by the purple line. Error bars indicate s.e.m. at each point. Right, distribution of distances between the MTOC and the center of the irradiated region (called a polarization histogram) for all observations after 4 min. Each experiment was 8 min in length. Curves were derived from at least 20 cells each. Data are representative of two independent experiments. (**b,c**) 5C.C7 T cells expressing GFP–Centrin-2 were loaded with the calcium indicator Fura-2AM and mixed with APCs in the presence of either 500 nM Gö6983 or vehicle control (DMSO). (**b**) Representative timelapse montages (0.5 min intervals) showing control (above) and Gö6983-treated (below) cells. Each GFP–Centrin-2 image is paired with a corresponding differential interference contrast (DIC) image. Ratiometric Fura-2 signal (warmer colors indicate higher intracellular Ca^{2+}) is overlaid on each DIC image. The relevant APC is colored blue in each GFP–Centrin-2 image. (**c**) Quantification of MTOC polarization. For each observation, the MTOC was assigned to one of four positional bins (left), generating a distribution of MTOC positions for the entire data set (right). A total of 15 DMSO-treated control cells (287 observations) and 9 Gö6983-treated cells (155 observations) were analyzed. Data are representative of one experiment.

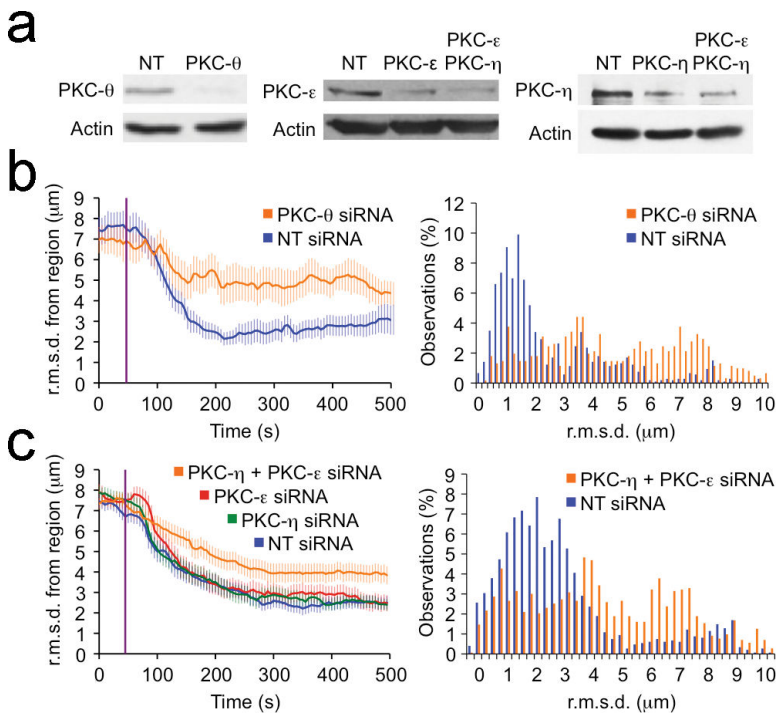

Figure 5.

PKC-θ and either PKC-ε or PKC-η are required for MTOC polarization. 5C.C7 T cells expressing GFP–Centrin-2 were nucleofected with siRNA against the indicated proteins and used for TCR photoactivation studies. (**a**) Immunoblot validation of PKC knockdown by siRNA. The proteins targeted by siRNA in each sample are listed above the blots, and the proteins detected by antibodies are listed to the left of the blots. NT = nontargeting siRNA control. (**b,c**) MTOC polarization in cells nucleofected with siRNA against PKC-θ (**b**) PKC-ε (**c**), PKC-η (**c**), or PKC-ε and PKC-η together (**c**). Average path and polarization histogram analyses were performed as described in **Fig. 4a**. All curves were derived from at least 12 cells. Data are representative of at least three independent experiments.

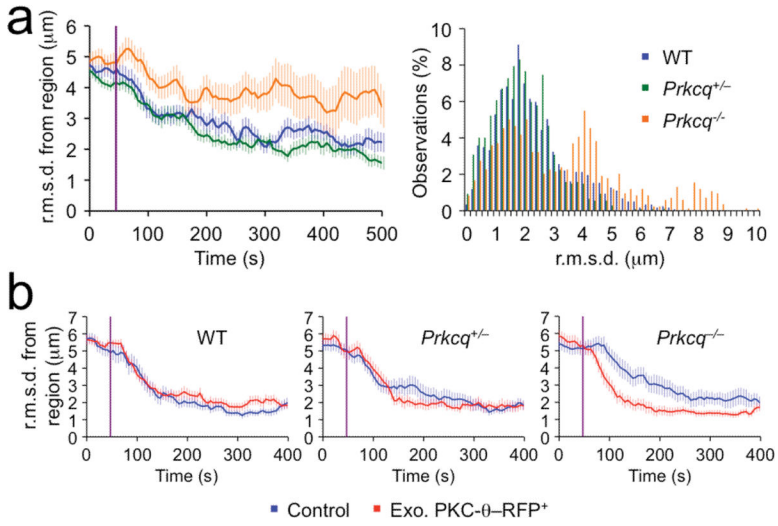

Figure 6.

Prkcq$^{-/-}$ T cells are defective in MTOC polarization. (**a**) TCR photoactivation experiments were performed using GFP–tubulin expressing 5C.C7 T cells derived from *Prkcq*$^{-/-}$ mice, *Prkcq*$^{+/-}$ littermate controls, or wild-type mice as indicated. Average path and polarization histogram analyses of MTOC reorientation were carried out as described in **Fig. 4a**. Curves were derived from at least 17 cells. Data are representative of two independent experiments in which cells were stimulated with ~50% less UV light than in typical photoactivation studies. (**b**) 5C.C7 T cells with the indicated PKC-θ genotype were transduced with exogenous (exo.) PKC-θ–RFP and used for TCR photoactivation studies. MTOC polarization in cells transduced with PKC-θ–RFP and in untransduced control cells was analyzed by average path as described in **Fig. 4a**. Curves were derived from at least 21 cells. Data are representative of three independent experiments.

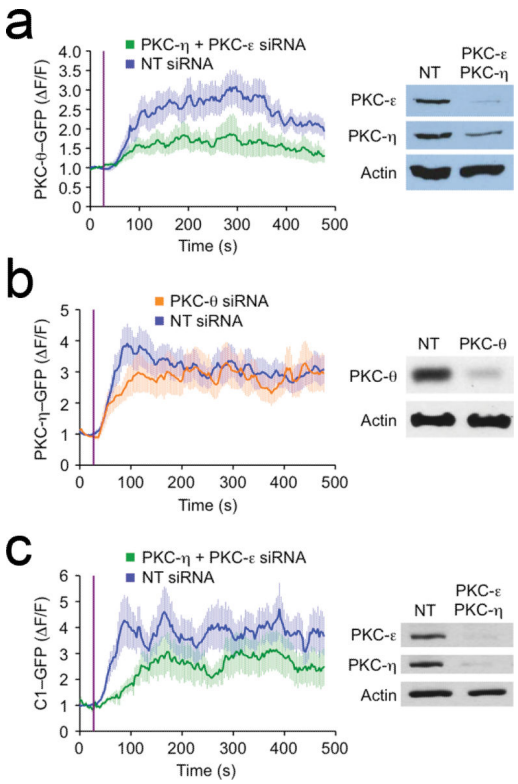

Figure 7.

PKC-ε and PKC-η are required for PKC-θ recruitment. 5C.C7 T cells expressing PKC-θ–GFP (**a**), PKC-η–GFP (**b**), or the C1 region of PKC-θ fused to GFP (C1–GFP) (**c**), were nucleofected with siRNA against the indicated proteins and used for TCR photoactivation studies. Left, normalized mean fluorescence intensity (ΔF/F) of the indicated GFP-labeled protein was plotted versus time, with UV irradiation indicated by the purple line. Right, immunoblot validation of PKC knockdown by siRNA. The proteins targeted by siRNA in each sample are listed above the blots, and the proteins detected by antibodies are listed to the left of the blots. NT = nontargeting siRNA control. All curves were derived from at least 13 cells. Throughout the figure, error bars = s.e.m. All data are representative of at least two independent experiments.

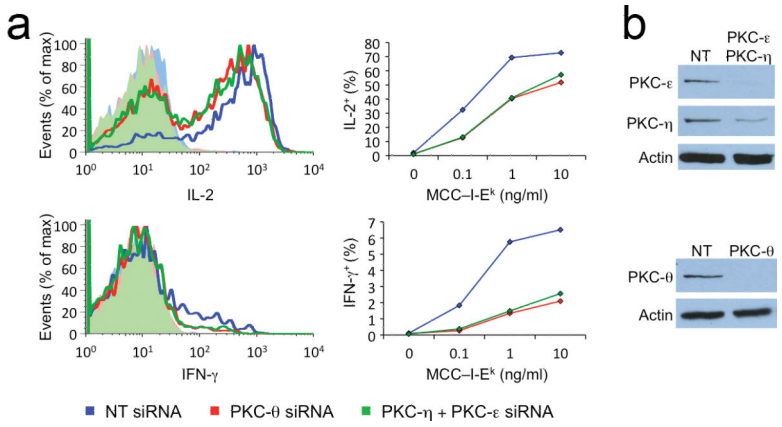

Figure 8.

PKC-θ, PKC-ε, and PKC-η are required for TCR-induced cytokine production. (**a**) 5C.C7 T cell blasts were nucleofected with the indicated siRNA duplexes and then stimulated with immobilized MCC–I-E^k. Left, histogram plots showing induced IL-2 (top) and IFN-γ (bottom) production quantified by intracellular cytokine staining. Unstimulated samples are graphed as shaded curves. Right, dose response curves showing the fraction of IL-2^+ (top) and IFN-γ^+ (bottom) cells as a function of the concentration of MCC–I-E^k used to prepare the stimulatory surface. Histograms on the left were derived from the 1 ng/ml MCC–I-E^k surfaces. (**b**) Immunoblot validation of PKC knockdown by siRNA. The proteins targeted by siRNA in each sample are listed above the blots, and the proteins detected by antibodies are listed to the left of the blots. NT = nontargeting siRNA control. All data are representative of at least two independent experiments.